Grid-Supportive Load Control for Residential ZIP Loads in DC Microgrid

Ömer Ekin[1], Giovanni De Carne[1], and Veit Hagenmeyer[1]

[1]Affiliation not available

January 20, 2025

Abstract

This paper introduces a novel control approach that equips inverter-based loads in low-voltage DC Microgrid with grid support capabilities, relying solely on local measurements. The approach is generalized for various load types—constant impedance (Z), constant current (I), and constant power (P)—collectively termed ZIP loads. Experimental validation on a real-world DC Microgrid setup demonstrates the superiority of the proposed method over conventional proportional-integral (PI) control, demonstrating improved voltage regulation and reliability.

Grid-Supportive Load Control for Residential ZIP Loads in DC Microgrid

Ömer Ekin, *Graduate Student Member, IEEE*, Giovanni De Carne, *Senior Member, IEEE*,
Veit Hagenmeyer, *Member, IEEE*

***Abstract*—This paper introduces a novel control approach that equips inverter-based loads in low-voltage DC Microgrid with grid support capabilities, relying solely on local measurements. The approach is generalized for various load types—constant impedance (Z), constant current (I), and constant power (P)—collectively termed ZIP loads. Experimental validation on a real-world DC Microgrid setup demonstrates the superiority of the proposed method over conventional proportional-integral (PI) control, demonstrating improved voltage regulation and reliability.**

***Index Terms*—DC Microgrid, Distributed Control, ZIP loads, Grid-Supportive Loads**

I. Introduction

THE rapid integration of renewable energy sources has significantly increased the need for flexibility in modern power systems. Traditionally, this flexibility has been achieved through energy storage systems and demand-side management strategies, such as load scheduling. However, automated demand response (ADR) mechanisms are emerging as a key solution, with controllable loads—referred to as grid-supportive loads (GSL) or grid-forming loads—playing a vital role in balancing supply and demand [1], [2]. Most demand-side management efforts traditionally focus on storage-based components. However, controllable loads have gained attention for their ability to dynamically adjust or curtail consumption without compromising functionality [1], [3], [4]. Among earlier contributions, Electric Springs (ES) [5], [6] have been widely recognized for their ability to stabilize voltage through the integration of non-critical loads and bidirectional DC/DC converters. While ES have demonstrated effectiveness in specific configurations, their reliance on additional power electronics can limit scalability and flexibility. Decentralized approaches (e.g., [7]) mitigate the challenges of centralized control by leveraging distributed optimization. However, their reliance on communication infrastructure introduces additional costs and vulnerabilities. In contrast, this paper proposes a communication-free control strategy that relies solely on local measurements, eliminating communication dependencies while maintaining robust grid-support capabilities. Although GSL has been extensively studied in AC systems [1]–[4], its application to DC Microgrids remains limited. Early research, such as [8], introduced GSL control for DC Microgrids but focused on simplified loads, lacked experimental validation, and ignored device-specific constraints, limiting practicality. To address these challenges, this paper proposes a novel communication-free grid-supportive control method for power electronics-interfaced loads in DC Microgrids. The key contributions of this work include:

(1) A communication-free GSL control method tailored for ZIP loads.
(2) A novel energy-based recovery and restoration strategy to enhance load management.
(3) Experimental validation of the proposed approach in a realistic DC Microgrid environment.

These contributions enhance DC Microgrid reliability, stability, and renewable energy integration.

This work has been supported by the Helmholtz Association under the program "Energy System Design" and under the Helmholtz Young Investigator Group "Hybrid Networks" (VH-NG-1613).

II. DC Microgrid System Description

The DC Microgrid consists of a Battery Energy Storage System (BESS), a photovoltaic (PV) array, and DC loads, as illustrated in Fig. 1. The BESS, connected via a bidirectional

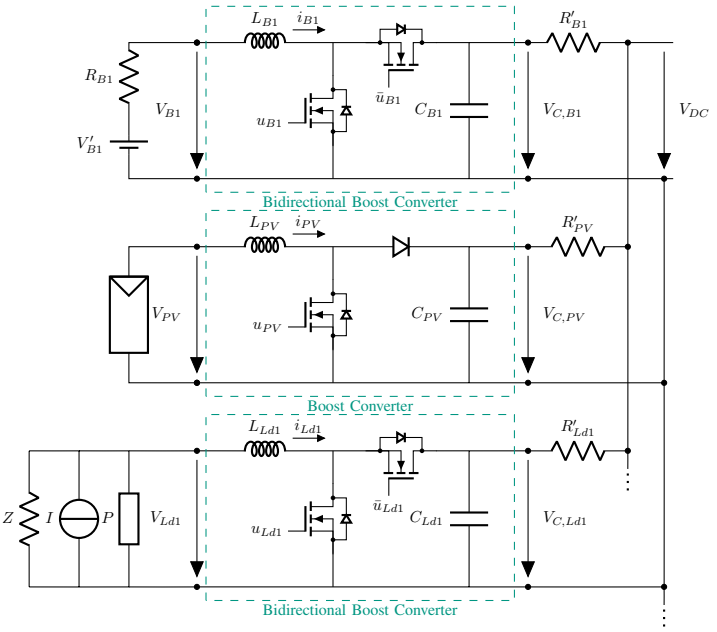

Fig. 1. Electrical circuit of the DC Microgrid configuration comprising a battery, photovoltaic system, and ZIP load.

boost converter, regulates the DC bus voltage, while the PV array uses a unidirectional boost converter with maximum power point tracking (MPPT) for power optimization. DC loads are interfaced through bidirectional buck converters to provide grid support. The AC front-end VSC employs vector current control to manage the interface with the AC grid. The dynamic behavior of the loads is modeled using averaged state-space equations, capturing their interaction with the DC grid:

$$\dot{I}_{Ldi} = \frac{1}{L_{Ldi}} V_{C_{Ldi}} u_{Ldi} - \frac{1}{L_{Ldi}} V_{Ldi} \tag{1}$$

$$\dot{V}_{CLdi} = \frac{1}{C_{Ldi} R'_{Ldi}} (V_{dc} - V_{CLdi}) - \frac{1}{C_{Ldi}} u_{Ldi} I_{Ldi} \tag{2}$$

where I_{Ldi} and V_{Ldi} represent the output current and voltage of the i^{th} load converter, respectively, and V_{CLdi} is the DC-side voltage of the load converter. The parameters L_{Ldi} and C_{Ldi} denote the inductance and capacitance of the load converter, while R'_{Ldi} is the equivalent resistance. The total load current includes contributions from constant impedance, constant current, and constant power components, collectively described as ZIP loads:

$$I_{Ldi} = \frac{V_{Ldi}}{Z_{Ldi}} + I_{\text{const}} + \frac{P_{\text{const}}}{V_{Ldi}} \tag{3}$$

The ZIP load model represents the voltage dependence of load power consumption and is mathematically expressed as:

$$P_{\text{Ldi}} = P_0 \cdot \Big(\underbrace{P_p}_{\substack{\text{const.} \\ \text{Power}}} + \underbrace{P_I \frac{V_{Ldi}}{V_0}}_{\substack{\text{const.} \\ \text{Current}}} + \underbrace{P_Z \left(\frac{V_{Ldi}}{V_0} \right)^2}_{\substack{\text{const.} \\ \text{Impedance}}} \Big) \tag{4}$$

where P_{Ldi} is the active power of the load, P_0 is the nominal active power at the nominal voltage V_0, and V_{Ldi} is the actual voltage at the load bus. The coefficients P_Z, P_I, and P_P correspond to the constant impedance, constant current, and constant power components, respectively, satisfying $P_Z + P_I + P_P = 1$. These coefficients can be provided by device manufacturers during the system design phase. This comprehensive modeling of ZIP loads allows for accurate representation of their dynamic behavior and supports the design of grid-supportive control strategies. This setup simulates a realistic DC Microgrid, enabling analysis of grid-supportive control in practical conditions.

III. Grid-Supportive Load Control

This section presents the proposed GSL control method, designed to enhance the grid-supportive capabilities of ZIP loads in DC Microgrids. The control method relies solely on local measurements and combines voltage-based modulation with a novel restoration strategy to achieve robust and adaptive load management. The overall control scheme is depicted in Fig. 2. The GSL concept consists of a GSL-based voltage function and a load restoration method.

A. GSL Voltage Control

The GSL control adjusts the reference voltage of the i^{th} load to modulate its power, mitigating DC bus voltage deviations in the Microgrid. The reference voltage is defined as [8]:

$$V^*_{Ldi} = V^{\text{nom}}_{Ldi} \cdot \xi_{Ldi} \tag{5}$$

where the scaling factor ξ_{Ldi} is determined by:

$$\xi_{Ldi} = \begin{cases} 1 + \sigma_i, & \text{if } \xi_i \geq 1 + \sigma_i, \\ 1 - \sigma_i, & \text{if } \xi_i \leq 1 - \sigma_i, \\ 1, & \text{if } (1 - \rho_i) \leq \xi_i \leq (1 + \rho_i), \\ \xi_i, & \text{otherwise.} \end{cases} \tag{6}$$

with

$$\xi_i = 1 + k_{\text{GSL}} \cdot \theta \cdot \left(\frac{V_{DC}}{V^*_{DC}} - 1 \right) \tag{7}$$

where σ_i defines the allowable percentage deviation in voltage for the i^{th} load (e.g. $\sigma_i = 0.05$ for a 5% variation), ρ_i sets a deadband to avoid frequent activations due to small fluctuations or noise, and $\theta \in (0, 1)$ is a recovery variable, regulating the gradual return of critical loads to their nominal state. A hysteresis is added to the deadband to improve stability and prevent oscillations near its boundaries. This method ensures precise load modulation, supporting the DC bus voltage maintenance during disturbances. For constant impedance and current loads, the control is effective. However, for constant power loads, a voltage reduction may increase current, potentially causing instability [9]. To address this, a generalized GSL control approach adjusts power dynamically using quadratic approximations of the ZIP load model. By applying the quadratic formula to Eq. (4), and assuming $P_Z \neq 0$ and $V_0 \neq 0$, the voltage V can be determined as follows:

$$\frac{V_{Ldi}}{V_0} = \frac{-P_I \pm \sqrt{P_I^2 - 4 \cdot P_Z \cdot \left(P_p V_0 - \frac{P_{\text{Ldi}}}{P_0} \right)}}{2 P_Z} \tag{8}$$

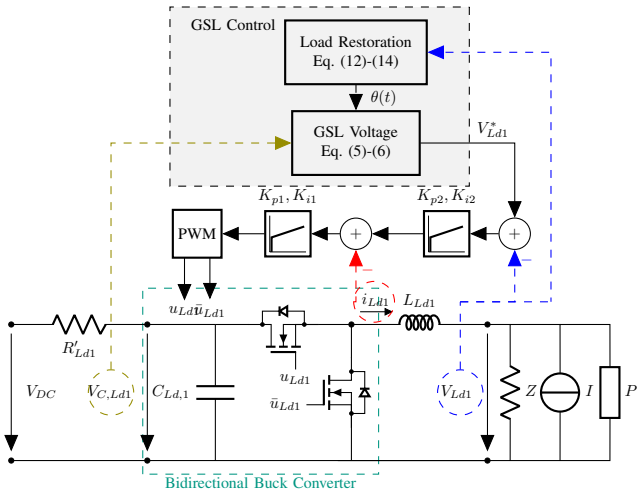

Fig. 2. Control scheme of GSL-based control with cascaded voltage and current PI and SoC estimation

where only the positive solution is physically meaningful. This expression accounts for the nonlinear interaction between power and voltage in ZIP loads, ensuring stability by dynamically regulating power components. By assuming $P_p = \text{const}$, $P_I \in [P_I^{\min}, P_I^{\max}]$, $P_Z \in [P_Z^{\min}, P_Z^{\max}]$ and $V_{DC} \in [V_{DC}^{\min}, V_{DC}^{\max}]$, the deviation in voltage and power is further incorporated into droop coefficients to modulate the load power dynamically:

$$m_I = \frac{P_I^{\max} - P_I^{\min}}{V_{DC}^{\max} - V_{DC}^{\min}}, \qquad m_Z = \frac{P_Z^{\max} - P_Z^{\min}}{V_{DC}^{\max} - V_{DC}^{\min}} \tag{9}$$

The power support through GSL method can be expressed as:

$$P_{Ldi}^* = P_P + P_I m_I (V_{DC} - V_{DC}^*) + P_Z m_Z (V_{DC} - V_{DC}^*) \tag{10}$$

By incorporating the GSL-modulated power terms into the Eq. (8), the modified expression becomes:

$$\frac{V_{Ldi}}{V_0} = \frac{-P_I}{2P_Z} + \frac{1}{\sqrt{2P_Z}} \Big(P_I^2 - \frac{4 \cdot P_Z \cdot (P_p V_0)}{P_0} - \frac{P_P + P_I m_I (V_{DC} - V_{DC}^*) + P_Z m_Z (V_{DC} - V_{DC}^*)}{P_0} \Big)^{\frac{1}{2}} \tag{11}$$

B. Load Restoration Control

Restoring critical loads after grid-supportive actions is essential to maintaining system stability and ensuring the continuous operation of vital loads. The proposed restoration strategy is energy-based, allowing for a smooth transition back to nominal operation while avoiding abrupt changes that could destabilize the grid.

1) Restoration Condition: The restoration process begins when the cumulative energy deviation exceeds a predefined threshold $E_{\text{GSL}}^{\max}$, as expressed by:

$$\underbrace{\Big(\int_{t-T_p}^{t} (P_{\text{GSL}}(\tau) - P_{\text{nom}}) d\tau}_{A_1} + \underbrace{\frac{T_{\text{res}}}{2} (P_{\text{GSL}}(t) - P_{\text{nom}})}_{A_2} \Big) > E_{\text{GSL}}^{\max} \tag{12}$$

where T_p represents the time window for integrating power deviations, and T_{res} the duration for gradual recovery to nominal power. $P_{\text{GSL}}(t)$ is the power of the GSL load at the time t and P_{nom} the nominal power. $E_{\text{GSL}}^{\max}$ is the maximum allowable energy deviation before initiating restoration. This condition ensures that recovery is triggered only when necessary, preventing premature actions and unnecessary stress on the system. The area A_1 corresponds to the measured energy deviation from past performance, while the area A_2 represents the estimated energy required to return to the nominal value. Assuming significantly faster voltage and current control (time-scale separation), ξ_{Ldi} can be used as a measurement variable for calculating relative deviations. This approach is advantageous because, for load ports that accommodate multiple loads, the nominal power is not inherently known.

$$\Big(\int_{t-T_p}^{t} (\xi_{Ldi}(t) - 1) d\tau + \frac{T_{\text{res}}}{2} (\xi_{Ldi}(t) - 1) > \Xi_{\text{GSL}}^{\max} \tag{13}$$

with $\Xi_{GSi}^{\max}$ being a normalized maximum permissible deviation of i^{th} load, which depends on the characteristics of the load. This inequality determines the load's recovery start.

2) Recovery Process: Once the restoration condition is met, the recovery process begins by gradually modulating the recovery variable θ from 1 to 0 over the recovery time T_{res}. This smooth transition prevents sudden changes in power, which could disrupt system stability. After the recovery period T_{rec}, the load operates at its nominal power for a defined interval before θ is ramped back to 1, fully restoring the load's grid-supportive functionalities. The evolution of θ during the recovery phase is depicted in Fig. 3 as:

① **Recovery Initiation:**

$$\theta(t) = 1 - \frac{t - t_{\text{start}}}{T_{\text{res}}}, \quad t \in [t_{\text{start}}, t_{\text{start}} + T_{\text{res}}], \tag{14}$$

where t_{start} is the time at which recovery begins.

② **Restoration Completion:** After the recovery phase, the load remains at its nominal state for T_{rec}.

③ **Re-enabling GSL Functionality:** The recovery variable θ is ramped back to 1, enabling the load to resume grid-supportive actions without additional adjustments.

IV. Experimental Setup and Results

The proposed GSL method has been experimentally validated through realistic DC Microgrid setup tests, as depicted in Fig. 4 comprising a 3 kW photovoltaic (PV) emulator, a 10 kW BESS Emulator, and ZIP loads with dynamically adjustable constant impedance, current, and power components. The line resistances in Fig. 1 are all approximately 0.1 Ω, while the capacitors are all 500 µF and the inductors are 2.5 mH. The performance of the proposed GSL method is evaluated by comparison with a standard Proportional-Integral (PI) control. In order to a consistent comparison between the two control approaches, the influence of weather variations on the PV emulator system is excluded by maintaining a constant irradiance and temperature. The DC bus operates at 700 V, with three load converters in the system. The first and second converters supply resistive loads of 4.4 kW and 1.8 kW, respectively. The third converter feeds a ZIP load with parameters $P_Z = 0.3$, $P_I = 0.2$, and $P_Z = 0.5$, and a nominal power of 1.75 kW. At $t = 0.1$ s, a 4 kW load is directly connected to the DC bus, resulting in a voltage drop. Fig. 5 illustrates the comparative performance of the control

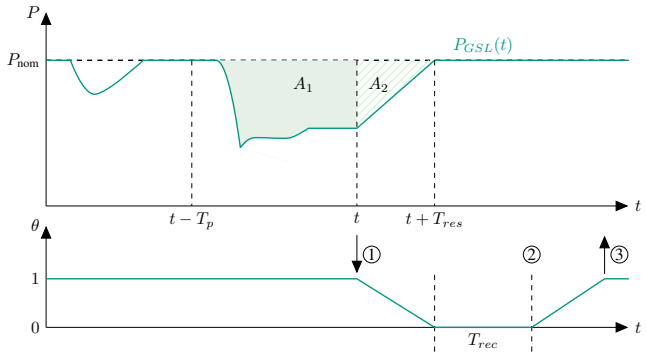

Fig. 3. Conceptual representation of the restoration method for critical loads in DC Microgrid over time. The function illustrates the gradual recovery and prioritization of critical loads following a disruption.

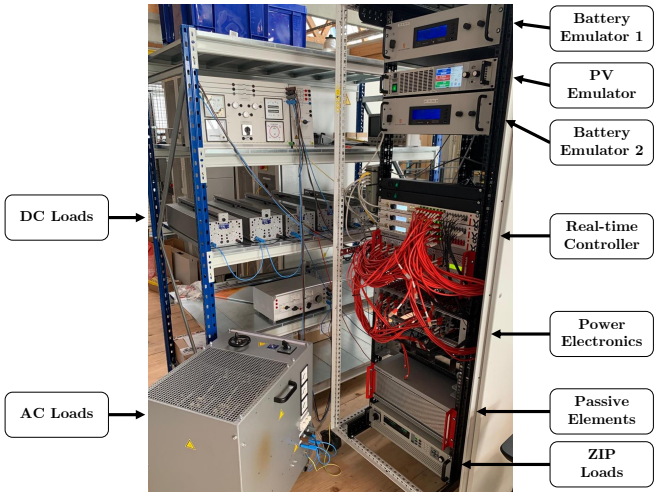

Fig. 4. DC Microgrid HW setup consisting of a PV emulator, inverter-based loads, real-time controller, SiC-Mosfets, passive components, Battery emulators, and a VSC interface the distribution grid

strategies: without GSL (blue), with GSL (orange), and with GSL and recovery (yellow). In Fig. 5(a), the voltage profiles show that the inclusion of GSL improves voltage dynamics, with further improvements observed when GSL with recovery is applied. Fig. 5(b), (c), and (d) depict the respective load powers for each case. In Fig. 6, the total load power is

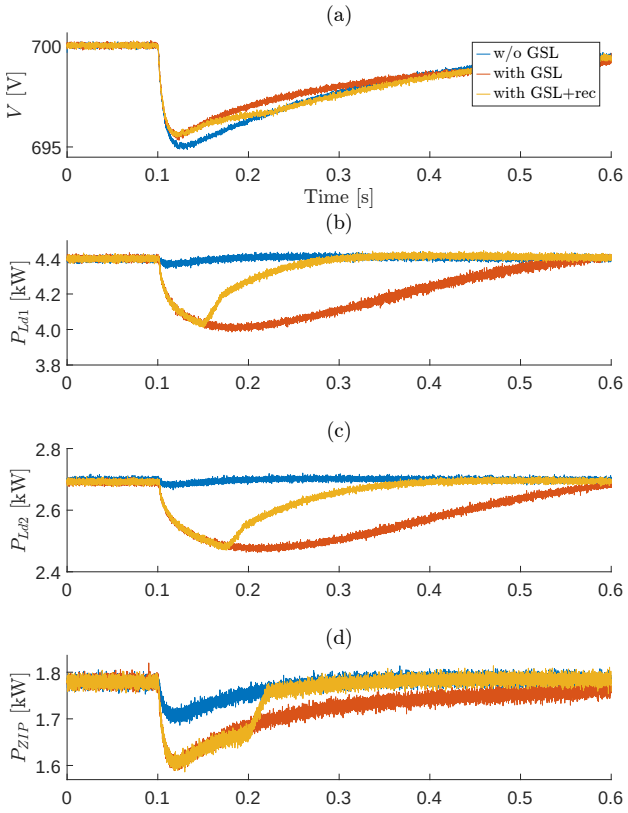

Fig. 5. Experimental results: without GSL (blue), with GSL (red), and with GSL and load recovery (yellow). Subfigures: (a) DC bus voltage, (b) load 1 power, (c) load 2 power, and (d) ZIP load power.

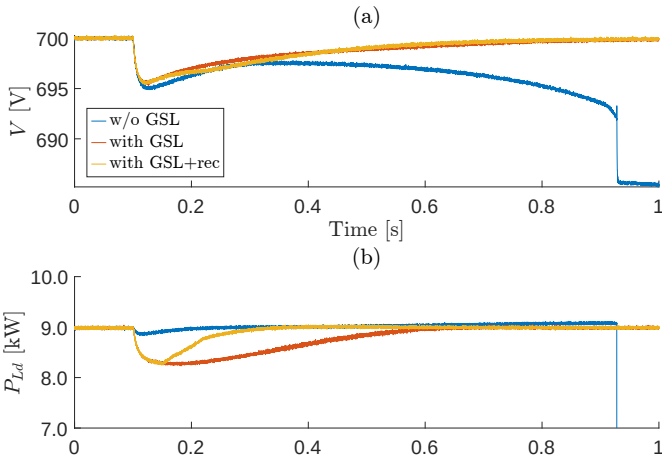

Fig. 6. Experimental results: without GSL (blue), with GSL (red), and with GSL and load recovery (yellow). Subfigures: (a) DC bus voltage and (b) total load power.

increased to 9 kW, and a 4 kW load step is introduced at $t = 0.1$ s. In this case, without GSL, the system fails due to the battery reaching its power limit. However, as demonstrated in Fig. 6, the inclusion of GSL enhances system reliability and prevents a system failure.

V. Conclusion and Outlook

This letter presents a novel GSL control method for DC Microgrids, with the feature to enable grid support services for ZIP loads. Experimental validation demonstrates improved voltage stability compared to existing methods. Future work will focus on scaling the method for larger systems and further analyzing its impact on stability.

References

[1] H. Jain, B. Mather, A. K. Jain, and S. F. Baldwin, "Grid-supportive loads—a new approach to increasing renewable energy in power systems," *IEEE Transactions on Smart Grid*, vol. 13, no. 4, pp. 2959–2972, 2022.

[2] O. Gomis-Bellmunt, S. D. Tavakoli, V. A. Lacerda, and E. Prieto-Araujo, "Grid-forming loads: Can the loads be in charge of forming the grid in modern power systems?" *IEEE Transactions on Smart Grid*, vol. 14, no. 2, pp. 1042–1055, 2023.

[3] Y. Son, M. Blonsky, N. Guruwacharya, V. R. Chowdhury, and B. Mather, "Autonomous grid support functionality in variable-speed drive-based end-use loads," *IEEE Transactions on Power Electronics*, vol. 39, no. 10, pp. 12 177–12 182, 2024.

[4] F. Albeladi and M. Barati, "Utilizing grid-supportive load response to shape resilient frequency control of the power grid," *IET Generation, Transmission & Distribution*, vol. 18, no. 2, pp. 388–400, 2024.

[5] X. Chen, M. Shi, H. Sun, Y. Li, and H. He, "Distributed cooperative control and stability analysis of multiple dc electric springs in a dc microgrid," *IEEE Transactions on Industrial Electronics*, vol. 65, no. 7, pp. 5611–5622, 2018.

[6] H. Yang, T. Li, Y. Long, C. L. P. Chen, and Y. Xiao, "Distributed virtual inertia implementation of multiple electric springs based on model predictive control in dc microgrids," *IEEE Transactions on Industrial Electronics*, vol. 69, no. 12, pp. 13 439–13 450, 2022.

[7] K. Sakurama and M. Miura, "Communication-based decentralized demand response for smart microgrids," *IEEE Transactions on Industrial Electronics*, vol. 64, no. 6, pp. 5192–5202, 2017.

[8] Ö. Ekin, A. Balakrishnan, L. Spatafora, and V. Hagenmeyer, "Distributed control strategy of grid supportive loads for DC microgrids," in *9th IEEE Workshop on the Electronic Grid (eGRID)*, in press.

[9] M. Gutierrez, P. A. Lindahl, and S. B. Leeb, "Constant power load modeling for a programmable impedance control strategy," *IEEE Transactions on Industrial Electronics*, vol. 69, no. 1, pp. 293–301, 2022.